Interfaces between Charged Surfaces and Ionic Liquids: Insights from Molecular Simulations

by Vladislav Ivaništšev and Maxim V. Fedorov

Interfacial effects in (room temperature) ionic liquids at charged surfaces are very important for ionic liquids applications in electrochemistry,[1] energy storage,[2] catalysis[3] and other areas (*e.g.*, lubrication[4,5]). However despite the many articles published on this subject (several hundred papers just in 2013) there is still no general agreement in the literature about the main factors that govern the structure and properties of ionic liquids at charged interfaces. This is mainly due to a large number of available combinations of ionic liquids (and their mixtures) and different surfaces. In this article, we make an attempt to rationalize recent experimental and computational findings on structural transitions in ionic liquids at charged interfaces. Herein, we present a critical (qualitative) analysis of available molecular modeling and experimental data using a recently developed concept of surface charge compensation that allows one to compare results for different ionic liquids on the same methodological footing.[6]

Molecular-Scale Interfacial Structure in Ionic Liquids

It has been shown in a number of experimental, modeling and theoretical studies that ionic liquids undergo structural changes at a molecular level upon charging of the solid-liquid interface. This has direct effects on mass and charge transfer phenomena occuring at the interface[7] as well as on the differential capacitance (C_{diff}) dependence on the electrode potential (U)[8–10] and temperature.[11,12] Changes in the interfacial structure of ionic liquids at charged surfaces also influence their lubrication properties.[13,14] Thus, from a practical point of view, the response of the interfacial ionic liquid structure to changes of the surface charge determines the performance of these interfaces in a variety of applications such as supercapacitors, batteries and electrocatalysis.[1–3] For recent reviews on experimental studies in this area we refer the reader to Refs. 15–17; for an overview of molecular modeling studies, please see Ref. 18.

Many independent experimental studies that have used different techniques (high-energy X-ray reflectivity, nuclear magnetic resonance, surface apparatus, and atomic force microscopy (AFM)) have reported the formation of multilayered structures of ionic liquids at charged interfaces with alternate layers of cations and anions (see *e.g.*, Refs. 19–22). Similar multilayered interfacial structures in ionic liquids have also been found in a number of Molecular Dynamics (MD) studies that have used different simulation methods (force fields and simulation conditions), ionic liquid models (coarse-grained and atomistic) as well as electrode models (carbon material, structure-less charged surface, metal, etc).[18]

It has been shown that charging of the electrode surface affects the magnitude of the ion layering at the interface.[8,9,13,14,23,24] Recent AFM studies have shown that the molecular-level structure and, consequently, interfacial properties of ionic liquids at charged surfaces can be changed by varying the surface potential.[13,14] It has also been shown in these studies that the interfacial structure can be changed by varying chemical composition of the ionic liquids, *i.e.* varying the length of alkyl chains of organic cations or anion type, etc.

However, we note that a multilayer-like structure is not the only possible arrangement of ions at the interface. Indeed, monolayer-like interfacial structures of ionic liquids at charged surfaces has been reported for several ionic liquids systems.[25] Critical analysis of several studies applying the sum frequency generation spectroscopy technique have led the authors to the conclusion that ions at the solid–liquid interface in ionic liquids are organized into essentially one ionic layer – a structure that resembles the classical Helmholtz picture of an ionic monolayer at a charged surface,[26] where the structural correlations between the ions beyond this layer resemble the bulk liquid structure.[25]

In trying to resolve the apparent contradiction between the different views on the interfacial structure of ionic liquids at charged surfaces, Kirchner *et al*. have recently performed an MD study of structural reorganization in ionic liquids upon surface charging using a wide scale of surface charges.[6] The authors of Ref. 6 used a coarse-grained model of ionic liquids that was previously developed in Refs. 8, 9. The results of this work have shown that by varying the surface charge, one can observe both multilayer structure and monolayer structure in ionic liquids. Although the conclusions were derived from a rather crude model that describes ionic liquid cations and anions as charged Lennard-Jones spheres, we believe that similar arguments can be applied when analyzing interfacial properties of more complex models and real systems.

Figure 1 schematically presents two main types of the molecular-scale structure of an electrified electrode–ionic liquid interface

(continued on next page)

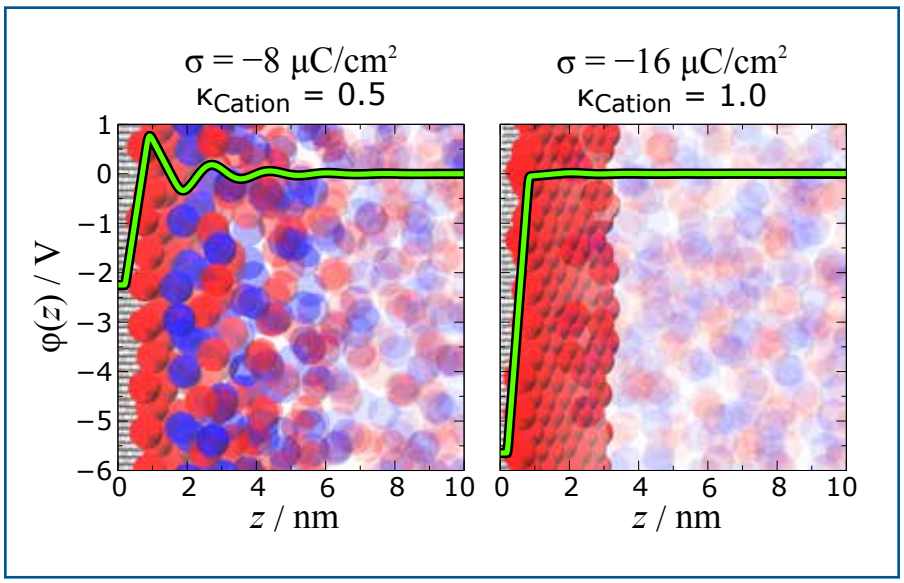

Fig. 1. *Electrostatic potential φ(z) across two model interfaces representing multilayer (LEFT) and monolayer (RIGHT) structures in a model ionic liquid. For the sake of simplicity, here both anions and cations are represented by spherical particles of the same size. In the underlying simulation snapshots the electrode, cations and anions are depicted as gray, red and blue spheres, respectively. The opacity level of the snapshots is adjusted proportionally to the variation of the amplitude of φ(z).*

that can be formed in a model ionic liquid: the multilayer structure (LEFT) and the monolayer structure (RIGHT).[27]

The multilayer structure in Fig. 1:LEFT is characterized by segregation of ions into cationic and anionic layers; this type of interfacial structure is related to the overscreening phenomena in ionic liquids.[8–10,28] Overscreening implies that the innermost layer contains more charge than is needed to compensate the surface charge (σ). The excess of charge in the innermost layer (λ_1, see the definition below) is compensated by subsequent ionic liquid layers in the transition region. The interfacial layering of ionic liquid particles is reflected in the oscillations of the electrostatic potential (φ(*z*) in Fig. 1), ionic number density (ρ_N in Fig. 2a), and ionic charge density and its derivatives, like the excess of charge in the *i*-th layer (λ_i in Fig. 2c). Thus, in the multilayer regime, the molecular-scale structure of ionic liquid at a charged interface can be divided into three regions: (i) the innermost layer of counter-ions in direct contact with the surface, (ii) the transition zone, several nanometers thick, that consists of alternating ion layers, and (iii) the bulk-like structured ionic liquid at larger distances from the surface.

We note that, in contrast to the multilayer regime, there is no transition zone in the case of the monolayer structure. Consequently there are no oscillations in the electrostatic potential (Fig. 1: RIGHT) – the innermost layer coexists directly with the bulk-like structured ionic liquid.

Surface Charge Compensation Phenomena

To perform a quantitative analysis of structural transitions in the interfacial region, we introduce a parameter θ^{max} that corresponds to the maximum charge density that can be stored in a monolayer for a selected type of ionic liquid ions (that would correspond to a densely packed monolayer of ions at physically possible maximum of ion packing density).[6]

By its definition, for a given ionic liquid θ^{max} depends only on the ion charge and geometric parameters of the selected ion type (size and shape).

The essential features of the *monolayer* structure are – (i) a linear electrostatic potential drop across the interface;[29] (ii) the charge density stored in the monolayer equals to θ^{max}; (iii) the electrode counter-ions that form the monolayer completely compensate the surface charge, *i.e.* $\sigma = \theta^{max}$. Due to the fact that θ^{max} depends only on the charge and geometry of the ions, one can use the surface charge renormalized by θ^{max} to compare different ionic liquid systems on the same universal footing. The dimensionless surface charge compensation parameter (κ) is then defined as:

$$\kappa_{Ion} = \left| \frac{\sigma}{\theta^{max}_{Ion}} \right|$$

Figure 2 illustrates the relationships between the structure of the transition region and packing of the innermost layer of counter-ions for different electrode charge densities.[27] Figure 2a shows the dependency of the ion number density (ρ_N) on the distance from the electrode (*z*) and the renormalized surface charge density – in the form of a contour map of $\rho_N(z, \kappa)$. As seen from this figure, vertical valleys divide the interface into the distinct regions discussed above: the innermost layer, the transition region and the bulk ionic liquid.

We note that the number of layers in the transition region (within ~1 to ~4 nm from the surface for the coarse-grained model) depends on the κ_{Ion}. It increases with increasing the surface charge until $\kappa_{Ion} \approx 0.5$ and then decreases revealing a bare monolayer at $\kappa_{Ion} = 1$. The horizontal valleys on the density contour map (Fig. 2a) at $\kappa_{Ion} = 1$ confirm the coexistence of the monolayer with bulk-like ionic liquid.

Molecular-Scale Structural Reorganization

For the sake of comparison of molecular organization in ionic liquids for the two regimes (multilayer *vs* monolayer), Fig. 2b shows anions (blue) and cations (red) within 1.7 nm from the charged surface at $\kappa_{Cation} = 0.5$ (TOP) and $\kappa_{Cation} = 1$ (BOTTOM). As can be seen from this figure, already at $\kappa_{Cation} = 0.5$ the innermost layer is dominated by the electrode counter-ions. In previous studies, observations of similar structures were associated with the lattice saturation effect and the maximum of the differential capacitance curve (C_{diff} vs. U).[30] However, Fig. 2 shows that within a distance of 1.7 nm from the electrode, there are also co-ions coordinated with several (2 to 4) counter-

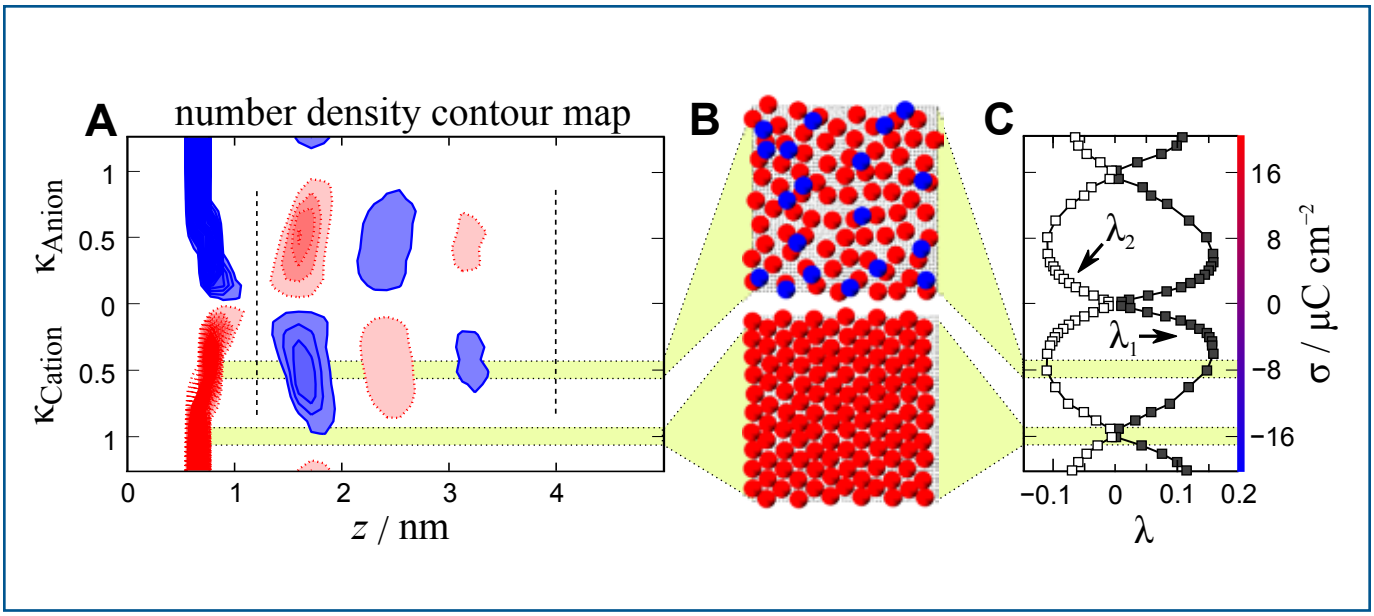

Fig. 2. *(a) Left: Dependency of anion (dark, blue) and cation (light, red) number density (ρ_N) on the distance from the electrode (z) and renormalized surface charge density (κ_{Ion}). Dashed lines divide the interface into the innermost, transition and bulk regions. The contour interval equals to ρ_{bulk}, the first contour starts at $1.5\rho_{bulk}$, and the $\rho_N(z,\kappa_{Ion})$ peaks are cut at $7.5\rho_{bulk}$ to facilitate the visual analysis. (b) Middle: The top subfigure shows dislocation of anions (blue) and cations (red) within 1.7 nm from the surface (gray) at $\sigma = -8$ μC cm^{-2} and $\kappa_{Cation} = 0.5$. The bottom subfigure shows dislocation of ions within 1.7 nm from the surface (gray) at $\sigma = -16$ μC cm^{-2} and $\kappa_{Cation} = 1$. (c) Right: Excess of charge in the first (λ_1, filled marks) and in the second (λ_2, empty marks) interfacial layers. The κ_{Ion} values of 1 correspond to ±16 μC cm^{-2} on the σ-scale shown on the left. Areas corresponding to the multilayer and monolayer structures are highlighted in color and with dotted lines.*

ions. Thus, we believe that the correlations between cations and anions actually define the distance between the counter-ions in the innermost layer at $\kappa_{Ion} = 0.5$.

The packing density of ions at the interface can be further increased upon surface charging without crowding up to the monolayer structure formation (from $\kappa_{Ion} = 0.5$ to $\kappa_{Ion} = 1.0$). To our best knowledge, the corresponding regime of electrostriction has not been previously described in the literature, although similar effects have been discussed before in terms of the C_{diff} vs. $|U|$ dependence.[28,31–33]

The transition from the multilayer structure to the monolayer structure is illustrated using the charge excess in the i-th layer (λ_i) in Fig. 2c. The parameter λ_i is defined through the cumulative charge density as follows:

$$\lambda_i = \kappa_{Ion} \times \left(\left| \frac{cn_Q(z_i)}{\sigma} \right| - 1 \right)$$

where z_i corresponds to an extremum (or a step height) of $|cn_Q(z)/\sigma|$ on the interval that defines the i-th layer. $cn_Q(z) = \frac{1}{A}\int_0^z \rho_Q(z')dz'$, where $\rho_Q(z) = \rho_N^{Cation}(z) \cdot q_{Cation} + \rho_N^{Anion}(z) \cdot q_{Anion}$ and A is a unit area. Thus the electrostatic potential $\varphi(z)$ Sas well as $\rho_Q(z)$, $cn_Q(z)$ and λ_i are all derived from the ion number densities at the interface. We note that the screening factor ($|cn_Q(z)/\sigma|$) as well as similar conceptions of the excess charge magnitude and the normalized surface charge density have been employed in several previous studies on ionic liquids at charged interfaces.[8,34–36]

The increase of the absolute charge excess in the interfacial layers with increasing κ_{Ion} from 0 to 0.5 manifests the transition from the disordered to the multilayer structure, while the further decrease of the charge excess after $\kappa_{Ion} = 0.5$ indicates the vanishing of the multilayer structure towards exposure of the monolayer structure at $\kappa_{Ion} = 1$. The λ_i vs. κ_{Ion} dependence represents an analog of dimensionless "reaction coordinate" for the reorganization process.

On the larger κ-scale, the monolayer structures in the coarse-grained models are formed at integer values of κ_{Ion} (adjusted for the compressibility of ions),[37] similar to the one-dimensional lattice Coulomb gas model (with lower fugacity).[38] An exact solution for the latter model also indicates that the maximal charge layering happens at renormalized surface charge densities of 0.5. The presented results reveal that similar effects can happen in three-dimensional ionic liquids models.

In the recent atomistic MD simulations of Paek *et al*. and Hu *et al*. there is evidence supporting monolayer formation in the case of more complex atomistic ionic liquid models (see Table II in Ref. 34 and Fig. 4 in Ref. 39). Therefore, in our opinion, the κ-scale can be used for rationalizing general trends in realistic systems. Figure 3 shows the relationship between the size of ions and the maximum packing charge density

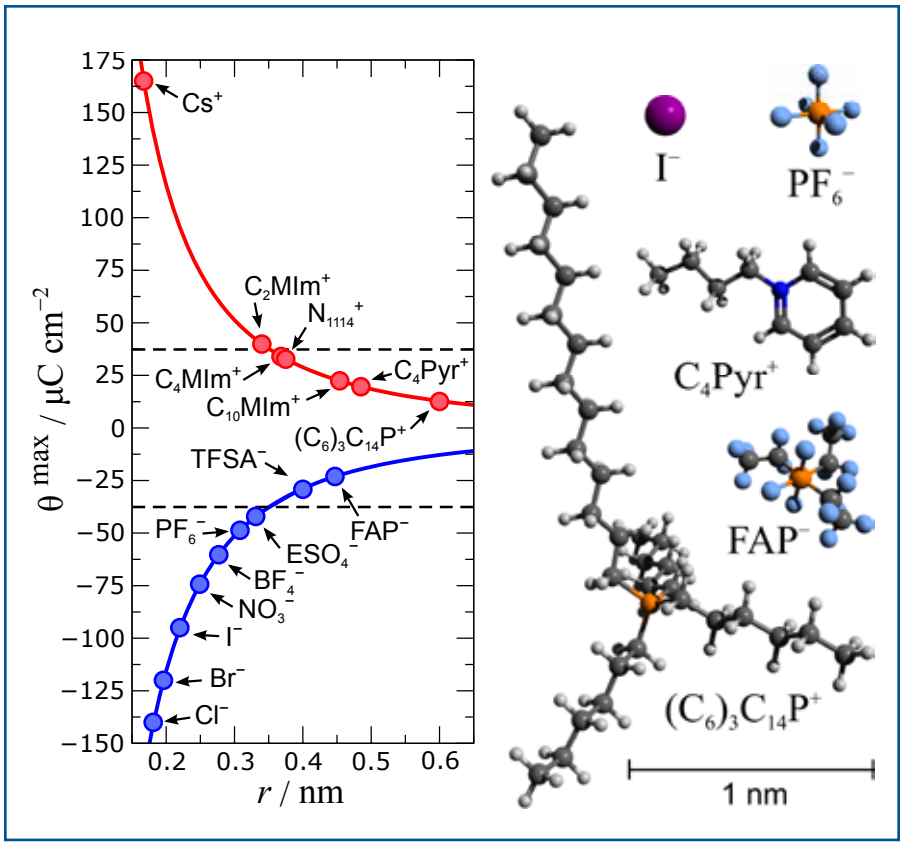

Fig. 3. *Left: Dependence of sterically determined maximum charge density (θ^{max}) on ionic radius (r). Dashed lines denote a range of surface charge densities commonly used in electrochemical experiments with ionic liquids. For complex ions the radii were estimated from their molecular volumes taken from Refs. 47, 48 assuming (as a first approximation) that ions are spherical in shape. The radii of halogenide anions and alkali metals cations were taken from Ref. 49. Right: ball-and-stick models of chosen ions amplified relative to the presented scale.*

in the ion monolayer θ^{max} (that corresponds to $\kappa_{Ion} = 1$). As a first approximation, it is assumed here that the ions are nearly round and are non-polarizable (we note that the former assumption is practically true for the alkali, halogenide and, perhaps, PF_6^- and BF_4^- ions). However, it should be noted that the presented θ^{max} values are quite approximate and can be adjusted by considering compressibility and specific packing of the ions.

According to the approximate ion-θ^{max} relationship presented on Fig. 3, the formation of the monolayer structure both in the cathodic and anodic regimes can be expected at realistic electrode charge densities (~±35 μC/cm²)[24,26] for a number of relatively large ions such as C_nMIm^+ and C_nMPyr^+ with $n \geq 4$, $TFSA^-$, FAP^-, etc. These ions are electrochemically stable due to the presence of stabilizing functional groups and larger contact distances from the electrode[40,41] and, therefore, relatively high electrode charge densities necessary for the formation of the monolayer structures can be achieved experimentally in these systems.

We note that the curve presented on Fig. 3 should be taken only as a *qualitative* guide because it does not take into account effects of complex geometric shapes of (some) ions, specific interionic interactions and (partial) charge transfer between the ions and the charged surface. These effects may change the specific conditions of the monolayer formation in realistic systems. Overall, the ideas discussed above require further development and an extensive validation by direct experiments and more sophisticated molecular models. Nevertheless, we note that a number of characteristic structures at electrochemical conditions have been observed experimentally that could serve as partial evidence of monolayer formation in real ionic liquid systems. For example, formation of ordered ionic adlayers has been observed via scanning tunneling microscopy;[42–44] a "monolayer" to "bilayer" restructuring induced by confinement has been observed by surface forces apparatus[45] and solid-like multilayers in ionic liquids have been recently reported.[22,46]

Conclusions

MD simulations of ionic liquid–electrode interfaces show that a transition from a multilayer ion structure to an ordered monolayer structure can be observed at certain values of the surface charge density. Upon this transition, a distinct change in the surface charge excess in the first two interfacial layers can be seen as a function of the renormalized surface charge density

(on the κ-scale). The degree of ordering in the innermost ion layer increases upon increasing the surface charge density, while the transition region exhibits systematic transformations upon surface charging. The point of maximum layering in the transition region depends on the density of the ionic liquid as well as on the ion-ion and ion–electrode interactions. For the coarse-grained ionic liquids models from Refs. 6, 8, 9 the point of the maximum layering is typically situated at $\kappa_{Ion} \approx 0.5$. This range of κ_{Ion} corresponds to frequently used surface charge densities in experimental and simulation studies on ionic liquids (see Fig. 3 as a guide) and this may explain the fact that multilayered structures in ionic liquids have often been reported in the experimental and modeling literature.[15-18] However, upon further increase of the charge density, the multilayer structure gradually transforms to a monolayer structure while approaching an integer value of κ_{Ion}. Herewith integer κ_{Ion} values serve as transition points for the structural reorganization processes happening in both regions. We suggest that the surface charge densities that correspond to $\kappa_{Ion} \approx 1$ (and consequently to the regime of monolayer formation) can be used as "landmark" points for qualitative and quantitative comparison of theoretical, simulations and experimental data on ionic liquids structure at charged surfaces.

Acknowledgments

We are grateful for computer time at the EPSRC funded ARCHIE-WeSt High Performance Computer (www.archie-west.ac.uk, EPSRC grant no. EP/K000586/1) and for the supercomputing support from the von Neumann-Institut für Computing, FZ Jülich (Project ID ESMI11). We thank Kathleen Kirchner, Tom Kirchner, Andrey Frolov, Alexei Kornyshev and Ruth Lynden-Bell for useful discussions.

About the Authors

Vladislav Ivaništšev is a Research Associate in the Department of Physics, the University of Strathclyde in Glasgow, UK (the Department is a part of the Scottish Universities Physics Alliance, SUPA). He received his PhD for his work on "Double layer structure and adsorption kinetics of ions at metal electrodes in room temperature ionic liquids" from the University of Tartu in 2012. His current research focuses on electrochemistry of ionic liquids and employs computer modeling. He may be reached at vladislav.ivanistsev@strath.ac.uk.

Maxim V. Fedorov is SUPA2 Professor (Chair) at the Department of Physics of the University of Strathclyde in Glasgow, UK (the Department is a part of the Scottish Universities Physics Alliance, SUPA). He received his PhD (2002, Biophysics) and DSc (2007, Physical Chemistry) degrees from the Russian Academy of Sciences. He moved to the University of Strathclyde in 2011 from the Max Planck Institute for Mathematics in the Sciences in Leipzig (Germany) where he was a research group leader. Since 2012 he is also Director of the West of Scotland Academia-Industry Supercomputer Centre (aka ARCHIE-WeST) in Glasgow (located at the University of Strathclyde). In 2012 he received the Helmholtz Award from the International Association of the Properties of Water and Steam (IAWPS) for his work on theoretical physical chemistry of liquids. His research interests focus on modeling of ionic liquids at electrified interfaces, ion effects on (bio) macromolecules and nano-objects, and molecular-scale theories of solvation interfaces. More details of his research can be found at http://bcp.phys.strath.ac.uk/molecular-theory-and-simulations/prof-maxim-fedorov. He may be reached at maxim.fedorov@strath.ac.uk.

References

1. M. Armand, F. Endres, D. R. MacFarlane, H. Ohno, and B. Scrosati, *Nat. Mater.*, **8**, 621 (2009).
2. D. R. MacFarlane, N. Tachikawa, M. Forsyth, J. M. Pringle, P. C. Howlett, G. D. Elliott, J. H. Davis, M. Watanabe, P. Simon, and C. A. Angell, *Energy Environ. Sci.*, **7**, 232 (2014).
3. P. Hapiot and C. Lagrost, *Chem. Rev.*, **108**, 2238 (2008).
4. J. Sweeney, F. Hausen, R. Hayes, G. B. Webber, F. Endres, M. W. Rutland, R. Bennewitz, and R. Atkin, *Phys. Rev. Lett.*, **109**, 155502 (2012).
5. O. Werzer, E. D. Cranston, G. G. Warr, R. Atkin, and M. W. Rutland, *Phys. Chem. Chem. Phys.*, **14**, 5147 (2012).
6. K. Kirchner, T. Kirchner, V. Ivaništšev, and M. Fedorov, *Electrochim. Acta*, **110**, 762 (2013).
7. F. Endres, O. Höfft, N. Borisenko, L. H. Gasparotto, A. Prowald, R. Al-Salman, T. Carstens, R. Atkin, A. Bund, and S. Z. El Abedin, *Phys. Chem. Chem. Phys.*, **12**, 1724 (2010).
8. M. V. Fedorov and A. A. Kornyshev, *Electrochim. Acta*, **53**, 6835 (2008).
9. M. V. Fedorov and A. A. Kornyshev, *J. Phys. Chem. B*, **112**, 11868 (2008).
10. M. Z. Bazant, B. D. Storey, and A. A. Kornyshev, *Phys. Rev. Lett.*, **106**, 046102 (2011).
11. M. Drüschler, N. Borisenko, J. Wallauer, C. Winter, B. Huber, F. Endres, and B. Roling, *Phys. Chem. Chem. Phys.*, **14**, 5090 (2012).
12. J. Vatamanu, O. Borodin, and G. D. Smith, *J. Am. Chem. Soc.*, **132**, 14825 (2010).
13. H. Li, M. W. Rutland, and R. Atkin, *Phys. Chem. Chem. Phys.*, **15**, 14616 (2013).
14. H. Li, F. Endres, and R. Atkin, *Phys. Chem. Chem. Phys.*, **15**, 14624 (2013).
15. R. Hayes, G. G. Warr, and R. Atkin, *Phys. Chem. Chem. Phys.*, **12**, 1709–1723 (2010).
16. S. Perkin, *Phys. Chem. Chem. Phys.*, **14**, 5052 (2012).
17. R. Atkin, N. Borisenko, M. Drüschler, F. Endres, R. Hayes, B. Huber, and B. Roling, *J. Mol. Liq.*, IN PRESS (2014).
18. C. Merlet, B. Rotenberg, P. A. Madden, and M. Salanne, *Phys. Chem. Chem. Phys.*, **15**, 15781 (2013).
19. M. Mezger, H. Schröder, H. Reichert, S. Schramm, J. S. Okasinski, S. Schöder, V. Honkimäki, M. Deutsch, B. M. Ocko, J. Ralston, M. Rohwerder, M. Stratmann, and H. Dosch, *Science*, **322**, 424 (2008).
20. Y. Yokota, T. Harada, and K.-I. Fukui, *Chem. Commun.*, **46**, 8627 (2010).
21. F. Endres, N. Borisenko, S. Z. E. Abedin, R. Hayes, and R. Atkin, *Faraday Discuss.*, **154**, 221 (2012).
22. M. R. Castillo, J. M. Fraile, and J. A. Mayoral, *Langmuir*, **28**, 11364 (2012).
23. R. M. Lynden-Bell, A. I. Frolov, and M. V. Fedorov, *Phys. Chem. Chem. Phys.*, **14**, 2693 (2012).
24. H. Zhou, M. Rouha, G. Feng, S. S. Lee, H. Docherty, P. Fenter, P. T. Cummings, P. F. Fulvio, S. Dai, J. McDonough, V. Presser, and Y. Gogotsi, *ACS Nano*, **6**, 9818 (2012).
25. S. Baldelli, *J. Phys. Chem. Lett.*, **4**, 244 (2013).
26. W. Schmickler and E. Santos, *Interfacial Electrochemistry*, 2nd ed., Springer, New York, (2010).
27. The simulation setup for the MD simulations and the model parameters are described in details in Refs. 6, 8, 9. The model systems consist of two smooth charged surfaces (11 nm×11 nm) and a variable number of ionic pairs (up to 1050).[6,8,9,37] Simulations were carried out using molecular dynamics at temperatures from 250 to 500 K, in an NVT ensemble. The results shown in Fig. 1 and 2 are drawn for the symmetric ionic liquid model with a bulk number density of 0.32 ions per nm^3 and ionic radii of 0.5 nm.
28. N. Georgi, A. A. Kornyshev, and M. V. Fedorov, *J. Electroanal. Chem.*, **649**, 261–267 (2010).
29. As Fig. 1 shows, in the case of the multilayer structure the total potential drop (in terms of its absolute values) is smaller than the drop in the first layer.

30. Y. Lauw, M. D. Horne, T. Rodopoulos, V. Lockett, B. Akgun, W. A. Hamilton, and A. R. J. Nelson, *Langmuir*, **28**, 7374 (2012).
31. A. A. Kornyshev, *J. Phys. Chem. B*, **111**, 5545 (2007).
32. Y. Lauw, M. D. Horne, T. Rodopoulos, and F. A. M. Leermakers, *Phys. Rev. Lett.*, **103**, 117801 (2009).
33. Y. Lauw, M. D. Horne, T. Rodopoulos, A. Nelson, and F. A. M. Leermakers, *J. Phys. Chem. B*, **114**, 11149 (2010).
34. E. Paek, A. J. Pak, and G. S. Hwang, *J. Electrochem. Soc.*, **160**, A1 (2013).
35. G. Feng, J. Huang, B. G. Sumpter, V. Meunier, and R. Qiao, *Phys. Chem. Chem. Phys.*, **13**, 14723 (2011).
36. J. Wu, T. Jiang, D.-E. Jiang, Z. Jin, and D. Henderson, *Soft Mat.*, **7**, 11222 (2011).
37. V. Ivaništšev, K. Kirchner, T. Kirchner, and M. Fedorov, *Phys. Rev. Lett.*, SUBMITTED (2014).
38. V. Démery, D. S. Dean, T. C. Hammant, R. R. Horgan, and R. Podgornik, *J. Chem. Phys.*, **137**, 064901 (2012).
39. Z. Hu, J. Vatamanu, O. Borodin, and D. Bedrov, *Phys. Chem. Chem. Phys.*, **15**, 14234 (2013).
40. G. H. Lane, *Electrochim. Acta*, **83**, 513 (2012).
41. S. Fletcher, V. J. Black, I. Kirkpatrick, and T. S. Varley, *J. Solid State Electrochem.*, **17**, 327 (2013).
42. Y. Su, J. Yan, M. Li, M. Zhang, and B. Mao, *J. Phys. Chem. C*, **117**, 205 (2013).
43. Y. Z. Su, Y. C. Fu, J. W. Yan, Z. B. Chen, and B. W. Mao, *Angew. Chem. Int. Edit.*, **48**, 5148 (2009).
44. G.-B. Pan and W. Freyland, *Chem. Phys. Lett.*, **427**, 96 (2006).
45. A. M. Smith, K. R. J. Lovelock, N. N. Gosvami, P. Licence, A. Dolan, T. Welton, and S. Perkin, *J. Phys. Chem. Lett.*, **4**, 378 (2013).
46. S. Bovio, A. Podesta, C. Lenardi, and P. Milani, *J. Phys. Chem. B*, **113**, 6600 (2009).
47. A. J. L. Costa, M. R. C. Soromenho, K. Shimizu, I. M. Marrucho, J. M. S. S. Esperança, J. N. C. Lopes, and L. P. N. Rebelo, *ChemPhysChem*, **13**, 1902 (2012).
48. M. Součková, J. Klomfar, and J. Pátek, *Fluid Phase Equilibr.*, **333**, 38 (2012).
49. D. R. Lide, Editor, *CRC Handbook of Chemistry and Physics*, 90th ed., CRC Press, New York (2009).